



ISSN: 0067-2904

Utilizing the Fundamental Nd: YAG Laser for the Pulsed Laser Ablation Approach to Synthesize Zinc Oxide Nanoparticles

Maryam M. Shehab¹, Eman K. jebur²

¹Department of Physics, College of Science University of Baghdad, Baghdad, Iraq ²Department of Physics, College of Sciences for Women, Baghdad University, Iraq

Received: 9/2/2024 Accepted: 29/8/2024 Published: 30/8/2025

Abstract

High-purity Zinc Oxide nanoparticles (ZnO NPs) were successfully synthesized using the pulse laser ablation technique. Low-power neodymium-doped yttrium aluminum garnet (Nd: YAG) laser was utilized as the energy source for the present study. A surface of a high-purity (99.95%) zinc plate submerged in 10 milliliters of water was exposed to a pulse laser beam of wavelength (λ =1064 nm), (τ = 9 ns). ZnO NPs in colloidal form were effectively synthesized. The characteristics of the nanoparticles were investigated using (XRD, SEM, Zeta Potential, and PL) approaches. XRD patterns revealed the hexagonal wurtzite structure of the nanoparticles. Was detected by XRD. The spherical form of the generated nanoparticle was seen in the SEM images of ZnO NPs. The photoluminescence spectrum showed two peaks of emission: one referring to band gap excitonic emission at 392 nm, the other at 512 nm has to do with the existence of oxygen vacancies that are singly ionized.

Keywords: pulsed laser ablation in water; ZnO NPs, (Nd: YAG) laser.

استخدام الطول الموجي الأساسي لليزر Nd: YAG ننهج الاستئصال بالليزر النبضي لتحضير جسيمات نانوبة لأوكسيد الزنك

 2 مریم ماجد شهاب 1* , ایمان کاظم جبور

¹علوم الفيزياء, كلية العلوم, جامعة بغداد, بغداد, العراق ²علوم الفيزياء, كلية العلوم للبنات, جامعة بغداد, بغداد, العراق

الخلاصة

تم تصنيع جسيمات أوكسيد الزنك النانوية عالية النقاء (ZnO NPs) بنجاح باستخدام تقنية الاستئصال بالليزر النبضي. تم استخدام ليزر (Nd: YAG) منخفض الطاقة كمصدر للطاقة لهذه الدراسة. تعرض سطح من صفيحة الزنك عالية النقاء (99.95%) المغمورة في 10 مليلتر من الماء لشعاع ليزر نبضي ذو الطول الموجي (1064) نانومتر، ومدة النبضة (9) نانوبانية. تم تصنيع ZnO NPs في شكل غرواني بشكل فعال ولها صبغة بنية شاحبة.)، تم فحص خصائص الجسيمات النانوية باستخدام طرق (XRD و SEM و PL Potential والمحاسية بواسطة . XRD يظهر الشكل الكروي للجسيمات النانوية المتولدة في صورة Zeta و Zno NPS يُظهر أطياف التلألؤ الضوئي ذروتين من الانبعاثات:

*Email: maryammajidshehab@gmail.com

أحدهما يشير إلى فجوة النطاق الانبعاث الإكسيتوني عند 392 نانومتر، والآخر عند 512 نانومتر، يتعلق بوجود وظائف الأوكسجين الشاغرة المتأينة بشكل فردى .

1- Introduction

Nanoparticles have a huge surface area-to-volume ratio that increases their thermal conductivity, chemical durability, non-linear optical performance, and catalytic activity [1]. Because of their ability to fight germs, nanoparticles are becoming more widely recognized as "nano antibiotics" [2]. Since nanoparticles are now used in various consumer industries, including those related to industry, health, food, space exploration, chemicals, and cosmetics, their synthesis must be done in an environmentally friendly way [3]. Metal oxide nanoparticles are currently been produced using a variety of physical and chemical methods. The environment and living things may be endangered by such production techniques, which are frequently pricy and labor-intensive. Consequently, a substitute for current nanoparticle production methods that are both affordable, secure, and ecologically friendly is required [4-6]. Zinc oxide nanoparticles (ZnO NPs) are multipurpose materials with distinctive strong chemical stability, high electrochemical coupling coefficient, a wide range of radiation absorption, and high photo-stability, which are examples of their physical and chemical characteristics [7,8]. They have enormous scientific and technical interests because of their extremely broadband gap energy (3.37 eV), good thermal and mechanical stability at ambient temperature, significant exciton-binding energy (60 meV), and prospective applications in electronics, optoelectronics, and laser technology [9,10]. ZnO Nps pyro-electric and piezoelectric properties make it suitable for use as a sensor, converter, energy source, and photo-catalyst for hydrogen production [11,12]. ZnO nanoparticles have been synthesized using various techniques, which can be classified as chemical or physical. Several techniques include spray conversion processing, sol-gel process, nanolithography, physical vapor deposition (PVD), chemical vapor deposition, and precipitation methods [13]. ZnO nanoparticles are of interest to biomedical and pro-ecological systems because of their low toxicity, biocompatibility, and biodegradability [14-16]. Metal oxide nanoparticles have undergone substantial research to determine their potential as an antibacterial agent. When nanoparticles are deposited on bacterial surfaces or when they build up in the cytoplasm or periplasm, membrane breakdown and disorder occur [10,11]. Antimicrobials function by adhering to negatively charged bacterial cell walls, which leads to altered permeability and instability of the cell envelope [17].

The main objective of this paper is to synthesize ZnO NPs employing the laser ablation approach and to investigate their physical properties and antibacterial activities.

2-Experimental details

3 (ml) of deionized water (DW) was added to the container containing the zinc oxide (ZnO) nanoparticles in the form of a disk. Following that, the container was placed on a rotating machine that rotated at 5 rpm and treated with Nd: YAG (1064 nm, 9 ns, 200 pulses, 6 Hz, and 500–700 mJ). A 100 mm focal length convex lens was employed. The disk's surface was affected by radiation, and ZnO NPs formed a colloidal solution.

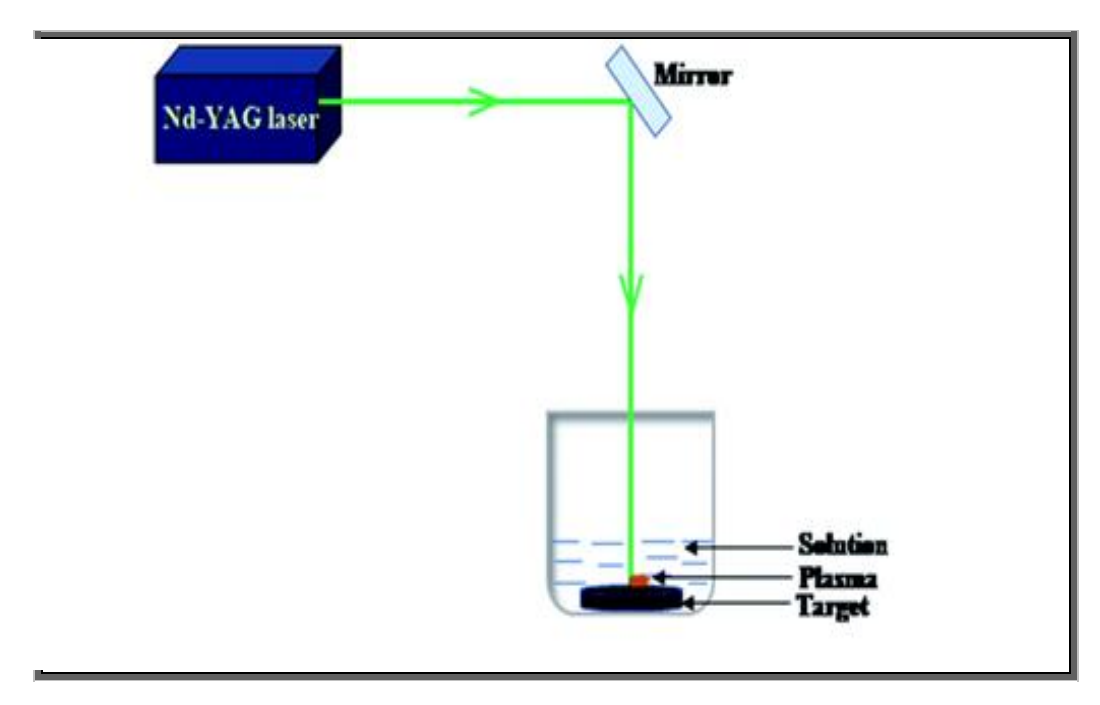


Figure (1): Schematic diagram of PLAL for NPs synthesized.

The optical and nanostructural characteristics of the synthesized ZnO nanoparticles were investigated. An X-ray diffractometer (ANALYTICAL) was used to record the ZnONPs X-ray diffraction pattern (XRD) using (Cu K α) radiation with a wavelength of 0.1541nm and a scan range of (2 θ = 20-90°). Scanning Electron Microscopy (SEM) was utilized to analyze the ZnO nanoparticles' composition and morphology. A fluorescence spectrophotometer (F-2500-Hitachi) was used to examine ZnO nanoparticles dispersed in water to determine their photoluminescence (PL)spectrum.

Klebsiella pneumoniae (a common type of bacteria), Staphylococcus (a Grampositive bacterium), Staphylococcus aureus (a gram-positive bacterium), Escherichia coli (a gram-negative bacterium), and Candida (genus of yeasts) were employed to test the antibacterial ability of the synthesized ZnO NPs.

The bacteria were grown in an agar medium in Petri dishes, and the synthesized ZnO NPs were tested to prevent the bacteria from growing. The process involved perforating the dishes and subsequently injecting them with a solution containing the particles. The plates were incubated for a whole day.

2-1 Inhibition test

disc diffusion tests were conducted to gauge the antibacterial treatments' effectiveness. At 37°C, Tryptic Soy Broth (TSB) was used to culture Staphylococcus aureus and Escherichia coli bacteria until they reached the late mid-log phase. A 50 L-sized bacterial sample was dispensed on each solid TSB agar plate. Then, sterile Whatman filter paper discs with a one-centimeter diameter were put on top of the tainted plates. The filter paper disc was then coated with 15 L of ZnO nanoparticles, which were allowed to rest for 24 hours at 37 °C. The inhibitory zone's diameter was then determined [18].

3-Results and Dissection

3.1. X-ray diffraction (XRD)

The crystallite size and crystalline structure of particles are frequently revealed by XRD analysis. Fig. (2) shows the XRD patterns of the prepared ZnONPS, which were prepared using Nd: YAG laser (λ =1064 nm) of different energies (500, 600, and 700 mJ) with 100 pulses. The figure shows the angles, Miller's index, and apparent crystal systems. The XRD patterns show several peaks representing the ZnO NPS according to [96-101-1260] ZnO JCDS Card, indicating a hexagonal pristine wurtzite crystal structure of the NPS when compared to the approved technique (JCDS Card Number [96-901-1600][19]. The figure shows the angles, Miller's index, and apparent crystal systems.

The figure depicts the biogenic produced for the ZnONPs' XRD pattern. The crystal planes (004), (102), (110), (103), (100), (101), (102), (110), and (103) are identified by the XRD peaks at $2\theta = 71.632^{\circ}$, 47.5808° , 56.6487° , 62.8917° , 31.8355° , 36.2871° , and 47.5808° , respectively. Using the Scherrer, Equation (1), the average particle size of the NPs was calculated[20]:

Where: λ is X-ray wavelength, 0.89 is Scherrer's constant, θ is the Bragg diffraction angle, and β is the Full Width at Half Maximum (FWHM).

Structural characteristics for ZnO NPs are shown in Table (2) and include Bragg angle (2 θ), Full Width at Half Maximum (FMHM), and the experimental inter-plane spacing (d) determined using Bragg's law Equation (2)[21-22]:

$$n\lambda = 2d \sin \theta$$
(2)

These results agree with the standard of X-ray diffraction data files JCPDS card No. 96-101-1260.

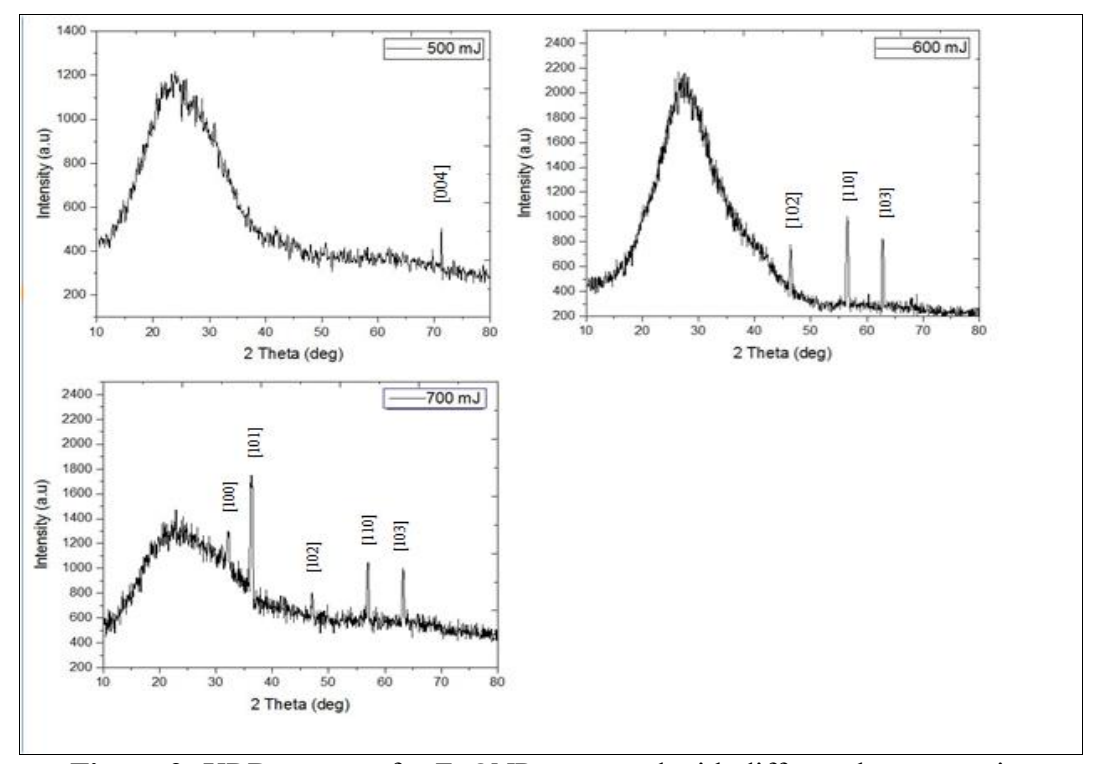


Figure 2: XRD patterns for ZnONPs prepared with different laser energies

Laser Material hkl **FWHM** 2THETA D Avg. d energy 500mJ 400 0.2819 71.632 34.79801 34.79801 102 0.2312 47.5808 37.63135 600mJ 110 0.2114 56.6487 42.76983 42.67113 103 0.1959 62.8917 47.6122 ZnO 100 0.1715 31.8355 48.28642 101 0.1622 51.66239 36.2871 700mJ 102 0.1586 47.5808 54.8573 55.29521 110 0.1535 56.6487 58.90256 103 0.1486 62.8917 62.76737

Table (1) the results of X-ray examination of ZnO NPS Synthesized with different laser energie

3.2. Scanning Electron Microscopy (SEM) analysis

Scanning electron microscopy (SEM) produces high-resolution images of a sample's surface and is used to evaluate the size, shape, and morphologies of created nanoparticles. Similar in operation to an optical microscope, a scanning electron microscope examines dispersed electrons from the material rather than photons. As a result, the SEM can produce images of up to 200.000 magnification. The equipment is highly helpful in identifying the size distribution of nanoparticles since it simultaneously allows for the creation of high-resolution surface images.

The synthesized ZnO NPs underwent SEM examination to ascertain their shape. The SEM images of the produced nanoparticles ablated in water are shown in Figs. (3) A, B, C. It can be seen that the particle size variation was evenly distributed. Additionally, the nanoparticles are smaller than 500 nm in size. Scanning electron microscope SEM analysis is employed to evaluate the dimensions, configuration, and structures of newly formed nanoparticles by producing detailed and high-quality images of the sample's surface.

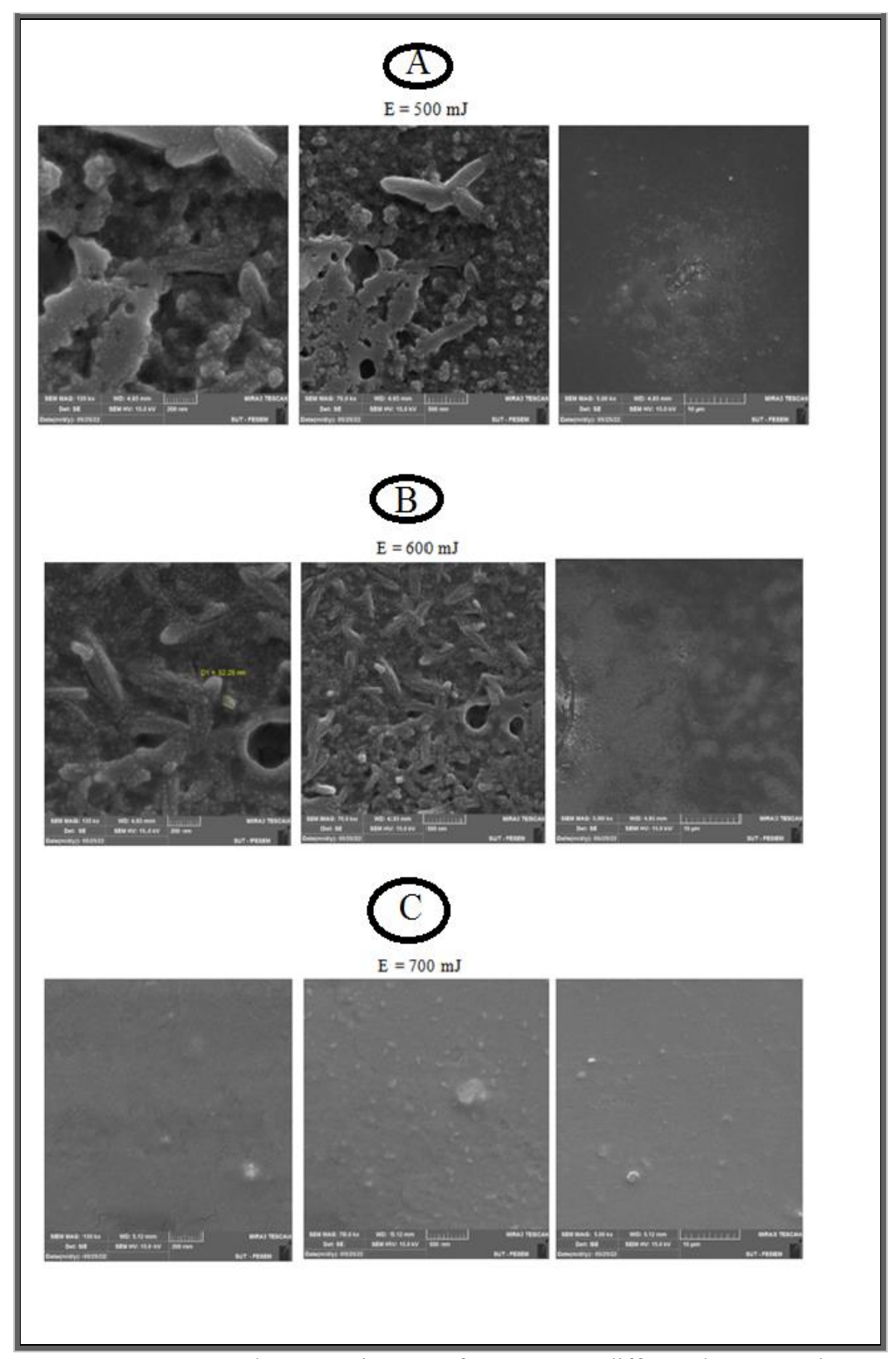


Figure 3: A, B, and C: SEM images of ZnO NPs at different laser energies.

3.3. Zeta Potential

Zeta potential examination helps determine the stability of nanoparticles in a solution. Zia potential is an indicator of the surface charge of particles and is a critical factor in preventing particles from clumping together. A higher voltage (either positive or negative) indicates

better stability of the particles in the solution. The synthesized ZnO NP's stability and surface charge were studied by a zeta potential analysis. This work revealed a colloidal solution's zeta potential value for ZnONPs of (-121, -68, and -34) mV for laser energies of 500, 600, and 700 mJ, respectively which demonstrated the nanoparticles' stability.

3.4. Photoluminescence Spectrum.

Noteworthy is the occurrence of a phenomenon called the "quantum size effect" when semiconducting materials are scaled down to the nanoscale region. Figure (4) depicts the photoluminescence spectrum for 392 nm excited ZnO nanopowder at room temperature. The spectrum shows two emission peaks: one from the near band gap excitonic emission at around 452 nm (UV area) and the other from singly ionized oxygen vacancies at about 512 nm [23-24]. The luminescence peak FWHM of the powder is only a few nanometers, demonstrating the spectrum's narrowly distributed nanoparticle size distribution.

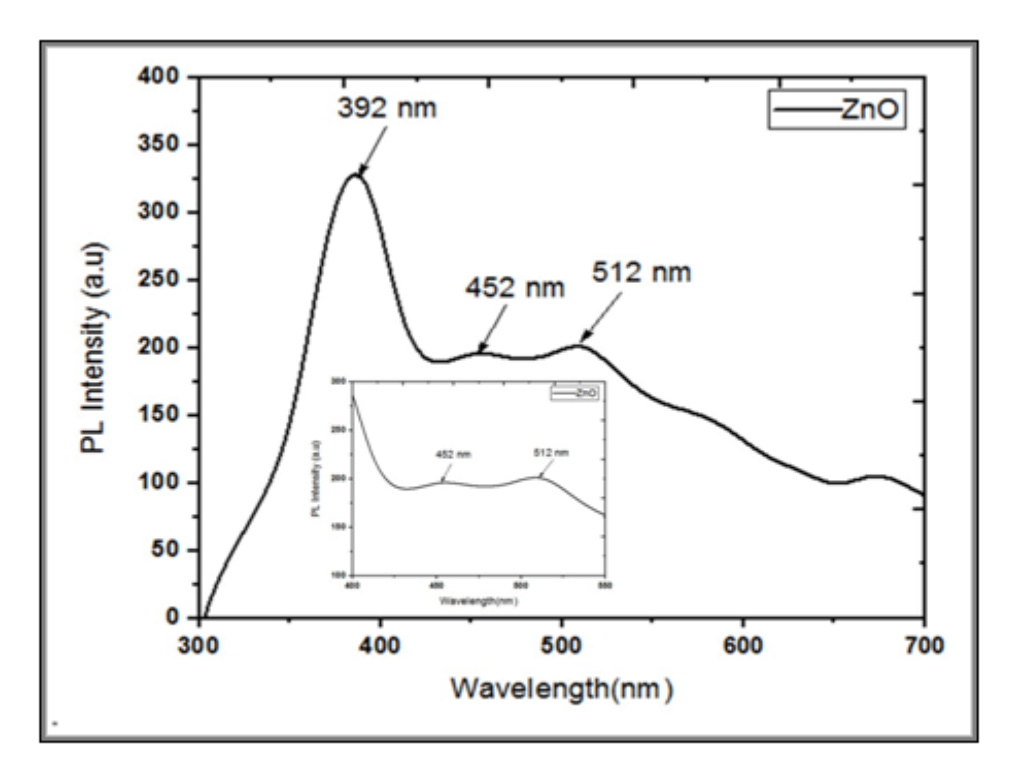


Figure (4) Photoluminescence spectrum of prepared ZnO NPS with different laser energies

5. Bio Applications:

The fabrication of zinc oxide nanoparticles (ZnO NPs) led to the creation of antibacterial agents that exhibit exceptional levels of activity. Figure 5 displays the analysis of using ZnO NPs prepared by different energies (500, 600, and 700 mJ) of the Nd:YAG laser for treating human multidrug-resistant illnesses caused by Klebsiella pneumoniae (a common type of bacteria), Staphylococcus (a Gram-positive bacterium), Staphylococcus aureus (a grampositive bacterium), Escherichia coli (a gram-negative bacterium). Candida (genus of yeasts) This was done in a clinical setting where the pathogens were isolated. Table 2 displays the measurement of the inhibitory region's diameter. The results revealed that S. aureus bacteria had a larger inhibitory zone than E. coli. One reason for this disparity is that the two bacteria cell walls structure is different. It was noted that the greatest diameter of the inhibition zone was for the nanoparticles synthesized using 700 mJ laser energy[26]. ZnO NPs synthesized using PLA of different laser energies exhibited antibacterial activity in comparably large levels. Since nanoparticles are so small, they can

break through the cells membrane of the bacteria disrupting the electron transport chain as well as the passage of energy across the membranes. As a result of this attack, a cell membrane's permeability is changed, and it is difficult to exert control over the passage of chemicals across the cytoplasmic membrane of the bacterial cell, ultimately resulting in the cell's death [25]. As a result, the creation of free radicals and the subsequent damage to the cytoplasmic membrane has been considered the basis for the antibacterial action of nanoparticles. It has been shown in several studies that nanoparticles may kill gram-negative bacteria by breaking through their cell wall.

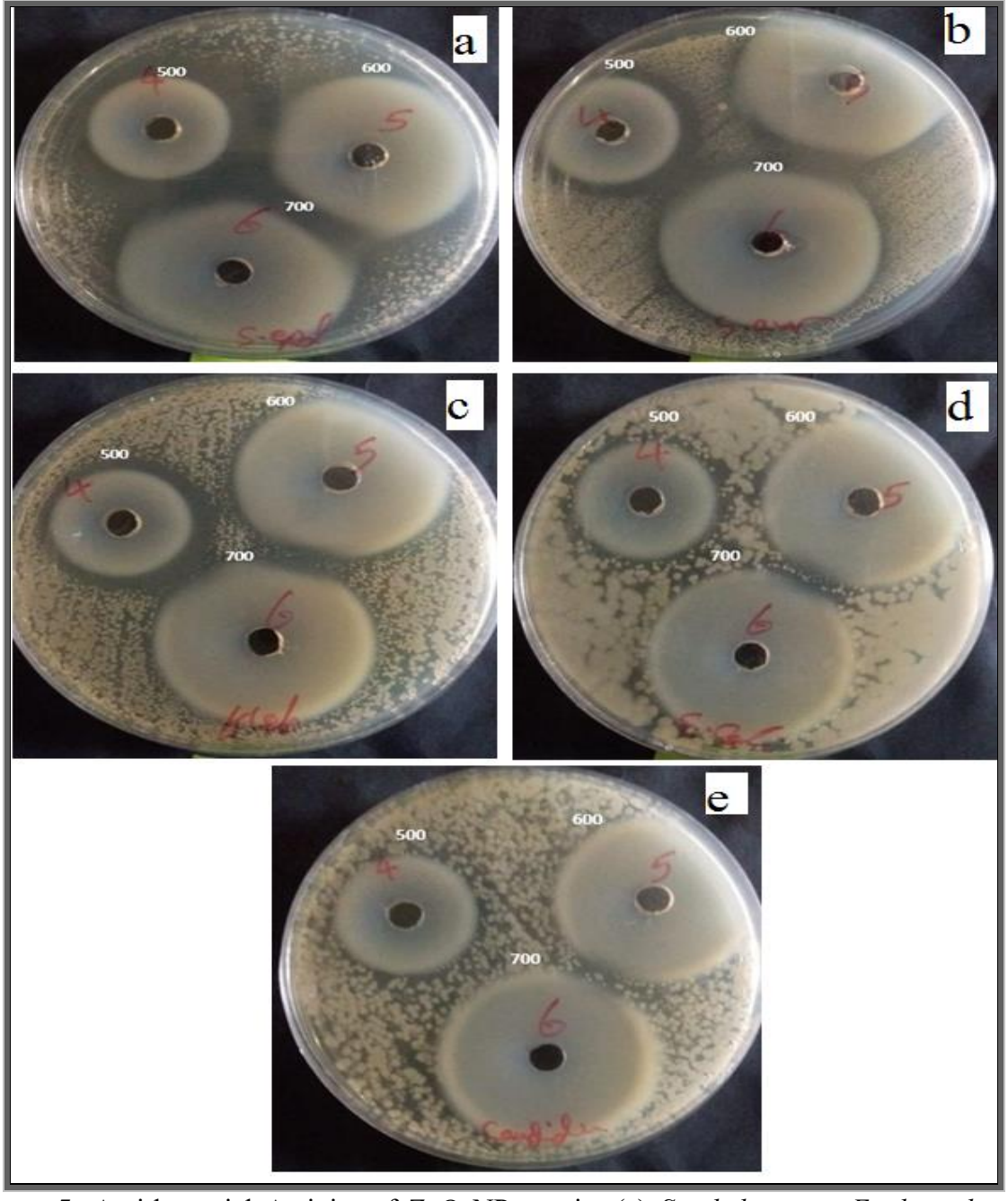


Figure 5: Anti-bacterial Activity of ZnO NPs against(a) *Staphylococcus Epidermidis, (b) Staphylococcus aureus, (c) Klebsiella Pneumonia, (d) Escherichia coli, and (e) Candida*

Name of the Microorganisms	Diameter of inhibition zone (mm)		
	ZnO NPs	ZnO NPs	ZnO NPs
	500 mJ	600 mJ	700 mJ
Staphylococcus. aureus	30	37	41
Staphylococcus. epidermidis)	30	45	45
E. coli	25	35	36
Klebsiella. pneumonia	30	38	35
candida	25	34	37

Table 2. Results of the antibacterial and anti-fungal activity of ZnO, NPs

4. Conclusion

Zinc oxide (ZnO) is recognized as a significant nanomaterial that has demonstrated efficacy in inhibiting the growth of bacteria and fungi. Zinc oxide (ZnO) possesses distinctive physicochemical qualities that enable it to effectively combat bacterial and fungal infections. It achieves this by many methods, such as the release of zinc ions and its contact with cellular membranes. These actions disturb the essential functions of microorganisms, leading to their inhibition or destruction. The features of ZnO show great potential for many applications in the domains of medicine and agriculture. ZnO can be utilized to improve protection against infection and enhance the safety of food and agricultural products.

Acknowledgments

We thank the University of Baghdad, College of Science, Department of Physics, and Plasma Physics Lab. for supporting this work.

REFERENCE

- [1] Shams Tabrez Khan, Javed Musarrat, and Abdulaziz A. Al-Khedhairy, "Countering drug resistance, infectious diseases, and sepsis using metal and metal oxides nanoparticles: current status," *Colloids and Surfaces B: Biointerfaces*, vol. 146, pp. 70-83, 2016.
- [2] Murali Sastry, et al. "Biosynthesis of metal nanoparticles using fungi and actinomycete," *Current science*, vol.85, pp. 162-170, 2003.
- [3] Peter Tumutegyereize, et al. "Effect of temperature fluctuation, substrate concentration, and composition of starchy substrates in mixture and use of plant oils as antifoams on biogas production," Environmental Progress & Sustainable Energy, vol. 38, no. 4, p.13115, 2019.
- [4] Doris Segets, Johannes Gradl, Robin Klupp Taylor, Vassil Vassilev, and Wolfgang Peukert. "Analysis of optical absorbance spectra for the determination of ZnO nanoparticle size distribution, solubility, and surface energy," *ACS nano*, vol. 3, no. 7, pp. 1703-1710, 2009.
- [5] X. Lou, H. S. Shen, and Y. S. Shen, "Development of ZnO series ceramic semiconductor gas sensors," J. Sens. Trans. Technol, vol. 3, no. 1, pp. 1-5, 1991.
- [6] E. M. İ. N. Bacaksiz, Mehmet Parlak, M. U. R. A. T. Tomakin, A. Özçelik, M. Karakız, and M. Altunbaş, "The effects of zinc nitrate, zinc acetate and zinc chloride precursors on investigation of structural and optical properties of ZnO thin films," Journal of Alloys and Compounds, vol. 466, no. 1-2, pp. 447-450, 2008.
- [7] Jun Wang, Jieming Cao, Baoqing Fang, Peng Lu, Shaogao Deng, and Haiyan Wang, "Synthesis and characterization of multipod, flower-like, and shuttle-like ZnO frameworks in ionic liquids," Materials Letters, vol. 59, no. 11, pp. 1405-1408, 2005.
- [8] Zhong Lin Wang, "Splendid one-dimensional nanostructures of zinc oxide: a new nanomaterial family for nanotechnology," ACS nano, vol. 2, no. 10, pp. 1987-1992, 2008.
- [9] Mariem Chaari, and Adel Matoussi, "Electrical conduction and dielectric studies of ZnO pellets," Physica B: Condensed Matter, vol. 407, no. 17, pp. 3441-3447, 2012.
- 1101 II Ozour "A comprehensive review of 7nO materials and devices" I April Phys. vol. 98 no.

- 41301, pp. 1-103, 2005.
- [11] Sayan Bhattacharyya, and A. Gedanken, "A template-free, sonochemical route to porous ZnO nano-disks,." Microporous and Mesoporous Materials, vol. 110, no. 2-3, pp. 553-559, 2008.
- [12] Bettina Ludi, and Markus Niederberger, "Zinc oxide nanoparticles: chemical mechanisms and classical and non-classical crystallization," Dalton Transactions, vol. 42, no. 35, pp. 12554-12568, 2013.
- [13] R. Kalaivani, M. Maruthupandy, T. Muneeswaran, A. Hameedha Beevi, M. Anand, C. M. Ramakritinan, and A. K. Kumaraguru, "Synthesis of chitosan mediated silver nanoparticles (Ag NPs) for potential antimicrobial applications," Frontiers in Laboratory Medicine, vol. 2, no. 1, pp. 30-35, 2018.
- [14] B. Srinivasa Rao, B. Rajesh Kumar, V. Rajagopal Reddy, T. Subba Rao, and G. J. C. L. Chalapathi, "Preparation and characterization of CdS nanoparticles by chemical co-precipitation technique," Chalcogenide Letters, vol. 8, no. 3, pp. 177-185, 2011.
- [15] Jianguo Zhou, Fengying Zhao, Yingling Wang, Yan Zhang, and Lin Yang, "Size-controlled synthesis of ZnO nanoparticles and their photoluminescence properties," Journal of luminescence, vol. 122-123, pp. 195-197, 2007.
- [16] Zahra Monsef Khoshhesab, Mohammad Sarfaraz, and Mohsen Asadi Asadabad, "Preparation of ZnO nanostructures by chemical precipitation method," Synthesis and Reactivity in Inorganic, Metal-Organic, and Nano-Metal Chemistry, vol. 41, no. 7, pp. 814-819, 2011.
- [17] JCPDS, Powder Diffraction File. "Alphabetical index." Inorganic Compounds, International Centre for Diffraction Data, Newtown Square, Pa, USA, 1977.
- [18] Niema, A. A. R., E. M. Abbas, and NKh Abdalameer. "Enhanced antibacterial activity of selenium nanoparticles prepared by cold plasma in liquid." *Digest Journal of Nanomaterials & Biostructures (DJNB)* vol. 16, No. 4, pp. 1479-1485, 2022.
- [19] Harfesh, Duha K., Nisreen Kh Abdalameer, and Eman K. Jebur. "Preparation and Physical Properties of Mg-Zn Nano-crystal by Laser-induced Plasma." International Journal of Nanoscience, vol. 21, No. 5, pp. 1-6, 2022.
- [20] Ghdeeb, Nadia Jasim, and Nisreen Kh Abdalameer. "Synthesis, characterization, and antimicrobial activity of CuO nanoparticles and CuO/Ag nanocomposites." *Applied Nanoscience* vol. 14, No. 2, pp. 401-409, 2024.
- [21] Aadim, Kadhim A., and Maryam M. Shehab. "Influence of Laser Energy on the Structural and Optical Properties of (CdO):(CoO) Thin Films Produced by Laser-Induced Plasma (LIP)." Iraqi Journal of Physics 19.49 (2021): 42-52.
- [22] Nisreen kh. Abdalameer, Huda M.J. Ali, Mirvat D. Majed, The effect of cold plasma generated from argon gas on the optical band gap of nanostructures, Kuwait Journal of Science, Vol. 51, Issue 2, pp. 1-6, 2024.
- [23] Atul Gupta, H. S. Bhatti, D. Kumar, N. K. Verma, and R. P. Tandon, "Nano and bulk crystals of ZnO: synthesis and characterization," Digest Journal of nanomaterials and biostructures, vol. 1, no. 1, pp. 1-9, 2006.
- [24] Y. Chen, C. Zuo, Z. Li, and A. Chen, "Design of ceria grafted mesoporous silica composite particles for high-efficiency and damage-free oxide chemical mechanical polishing," J. Alloys Compd., vol. 736, pp. 276–288, 2018.
- [25] Tawfeeq, H. K., Abdalameer, N. K., Jassim, R. H., & Shehab, M. M. "Silver Nanoparticles Synthesized by Cold Plasma as an Antibiofilm Agent against Staphylococcus epidermidis Isolated from Acne". Nano Biomedicine & Engineering, vol. 16, No. 1, pp. 101-109, 2024.
- [26] Shatha Sh. Batros, Mohammed H. Ali, and Ali J. Addie, "Microstructure-Modulated Antibacterial Performance of Chemically Precipitated SnO2 Nanoparticles," Journal of Applied Sciences and Nanotechnology, vol. 3, No. 4, pp. 20-32, 2023.